# Research on modeling and predicting of BDS3 satellite clock bias using the attention mechanism-based LSTM (AttLSTM) neural network model

Jiaxing Li[1], Kaifei He[1, *], Tülay Kaya Eken[2], Haluk Özener[2], Xiang Xu[1], Xiaopeng Lu[3], Kai Ding[1,4], Xuchen Ma[1]

1. College of Oceanography and Space Informatics, China University of Petroleum (East China), Qingdao 266580, China

2. Kandilli Observatory and Earthquake Research Institute (KOERI), Boğaziçi University, Istanbul 34684, Turkey

3. Huzhou Spatial Planning Compilation and Research Center, Huzhou 313000, China

4. Shandong Vocational College of Information Technology, Weifang 261061, China

* Corresponding author: Kaifei He, kfhe@upc.edu.cn

**Abstract:** In the Global Navigation Satellite System (GNSS), the satellite clock bias (SCB) plays an important role in the application of real-time precise point positioning (RT-PPP). Based on the operation of Beidou satellite global service, it is very important to establish a reliable Beidou SCB prediction model. In this research, an attention mechanism-based long short-term memory neural network (AttLSTM) model is applied to SCB prediction. The attention mechanism introduced in modelling can make the model pay less attention to useless information through weight allocation. In this paper, the BeiDou-3 Navigation Satellite System (BDS-3) satellite precision clock product provided by GFZ is used for clock prediction experiments. The proposed AttLSTM model, long short-term memory neural network (LSTM) model and quadratic polynomial (QP) model are compared and evaluated, and 12h and 24h SCB prediction experiments of BDS-3 satellite are set up. The results show that AttLSTM model can achieve high SCB prediction accuracy, and the averaged prediction accuracy of 12h and 24h can reach 1.41ns and 1.75ns. Compared with LSTM and QP models, the prediction accuracy of AttLSTM model is improved by 26.1%, 38.4% for 12h and 29.1%, 43.1% for 24h, respectively. Then, the clock bias predicted by the three models is applied to the static PPP positioning experiment, respectively. Through the analysis of the positioning results of 15 MGEX stations, the averaged positioning accuracy of AttLSTM model in the East, North and Up directions can reach 0.074m, 0.019m and 0.154m, respectively. Compared with LSTM and QP models, the positioning accuracy of AttLSTM model is improved by 42.5% and 44.4% in the East direction, 44.7% and 58.9% in the North direction, and 21.7% and 21.8% in the Up direction.

**Key words**: BDS-3 satellite; Satellite clock bias prediction; Long short-term memory neural network; Attention mechanism; PPP

## 1. Introduction

In global navigation satellite system (GNSS), the accuracy of real-time precise point positioning (RT-PPP) largely depends on the precise orbit and clock bias of the satellite. Providing users with high precision real-time products is the key to realize RT-PPP [1, 2]. At present, the accuracy of the

ultra-rapid orbit is about 5cm, but the accuracy of the ultra-rapid satellite clock is about 3ns, which cannot meet the requirements of RT-PPP [3]. Since 2013, the real-time service (RTS) has been launched by the International GNSS Service (IGS), which uses the network to provide users with real-time orbit and clock correction [4]. At present, RTS data stream products have been widely used in RT-PPP and other aspects, but there are still some problems such as time delay, data interruption and incomplete correction information [5-9]. For users, when RTS data transmission is interrupted due to poor communication status, it will seriously affect the application of RT-PPP [10]. Therefore, it is crucial to explore the prediction method of satellite clock bias to meet the requirements of RT-PPP.

Currently, the common satellite clock bias prediction models include quadratic polynomial (QP) model [11], grey model [12], Kalman filter model [13] and so on. These prediction models have certain defects. The QP model is sensitive to outliers, which will affect the prediction results [14]. Grey model is only suitable for short- and medium-term prediction and exponential growth prediction [15]. The Kalman filter model cannot achieve the optimal estimation effect in the nonlinear process [16, 17]. In addition, satellite clock bias of the BeiDou-3 Navigation Satellite System (BDS-3) completed in July 2020 [18] has complex characteristics, and the prediction accuracy can still be improved. The BDS-3 satellite has three orbit types: GEO, IGSO and MEO. Compared to MEO satellite, GEO and IGSO satellite clock bias have different periodic terms. Compared with GPS satellite clock bias, BDS satellite clock bias has an obvious nonlinear system bias. However, neural networks are more sensitive to nonlinear problems and can overcome the limitations of traditional models to achieve more accurate predictions. The wavelet neural network model was applied to satellite clock bias prediction, and it proved its reliability in clock bias prediction [19]. The long short-term memory network (LSTM) model was applied to satellite clock bias prediction by He et al. (2023), and the results show that the LSTM model has more obvious advantages than the QP model and

ARIMA model in clock bias prediction [20].

In order to improve the prediction accuracy of deep neural networks (DNN), the attention mechanism has been developed [21]. Attention mechanism was originally used in the field of computer vision [22]. It can reduce the attention of the model to useless information and emphasize the role of important features through weight allocation. And many studies have proved that the attention mechanism can improve the prediction accuracy and reliability of time series modelling [23-25]. Therefore, an attention mechanism-based long short-term memory neural network (AttLSTM) model is applied to SCB prediction in this study. Additionally, the AttLSTM model, LSTM model and QP model are compared and analysed in the clock bias prediction performance of BDS-3 satellite, and 15 MGEX stations are used to verify the usability of the clock bias prediction model in PPP applications.

## 2. Attention mechanism-based LSTM neural network

The proposed AttLSTM model, which uses the attention mechanism to adaptively find the key features in the input sequence, is applied in the BDS-3 satellite clock bias prediction. In this section, the model will be described in detail.

### 2.1 LSTM neural network

LSTM neural network model is a special recurrent neural network, which can solve the problem of gradient disappearance and gradient explosion in traditional neural networks [26]. The LSTM cell architecture is shown in Figure 1. Each cell of the LSTM model has several gates: input gates $i_t$, forget gates $f_t$, and output gates $O_t$. The input gate controls how much information can flow into the memory cell, the forget gate controls how much information flows from the previous memory cell into the current memory cell, and the output gate controls how much information flows from the current memory cell into the hidden state.
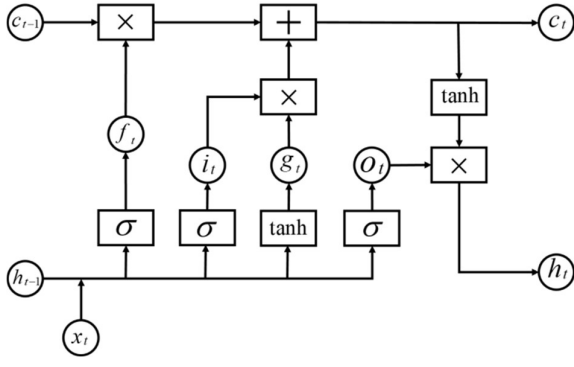
**Fig.1 the architecture of a LSTM cell**

The LSTM network introduces an internal state that then controls the transfer of information through input gates, forget gates and output gates. In the input gate, the input part is the matrix $[h_{t-1}, x_t]$, which consists of two parts. $h_{t-1}$ is the network input at the previous time instant, and the $x_t$ represents the network input at the current time instant. The weight matrix $W_i$ of the input gate, corresponding to the weights of the input part, is also composed of two parts, and the bias term of the input gate is $b_i$. Then the output $i_t$ of the input gate is calculated as follows:

$$i_t = \sigma(W_i \cdot [h_{t-1}, x_t] + b_i) \qquad (1)$$

If we look at the forget gate, the input part of the forget gate is also $[h_{t-1}, x_t]$. The weight matrix $W_f$ of the forget gate is also composed of the corresponding weights, and the bias term of the forget gate is $b_f$. Then the output $f_t$ of the forget gate is calculated as follows:

$$f_t = \sigma(W_f \cdot [h_{t-1}, x_t] + b_f) \qquad (2)$$

In the output gate, the input part is again $[h_{t-1}, x_t]$. The weight matrix $W_o$ of the output gate is also composed of the corresponding weights, and the bias term of the output gate is $b_o$. Then the output $O_t$ of the output gate is calculated as follows:

$$O_t = \sigma(W_o \cdot [h_{t-1}, x_t] + b_o) \qquad (3)$$

The input to calculate the temporary cell state $g_t$ is again $[h_{t-1}, x_t]$. The weight matrix is $W_g$, the activation function is the *tanh* function, and the bias term is $b_g$. Then the calculation equation of $g_t$ is as follows:

$$g_t = tanh(W_g \cdot [h_{t-1}, x_t] + b_g) \qquad (4)$$

The cell state $c_t$ is jointly determined by $f_t$, $c_{t-1}$, $i_t$ and $g_t$. The operator $\odot$ is the elementwise multiplication. And $c_t$ is calculated as follows:

$$c_t = f_t \odot c_{t-1} + i_t \odot g_t \qquad (5)$$

Finally, the final output value $h_t$ of the LSTM network can be calculated as follows:

$$h_t = O_t \odot tanh(c_t) \qquad (6)$$

**2.2 Attention mechanism**

Attention mechanism was originally used in the field of computer vision, which can reduce the model's attention to useless information and emphasize the role of important features through weight allocation [27, 28]. The architecture of attention mechanism is shown in Figure 2.



**Fig. 2 the architecture of attention block**

Attention mechanism is essentially a weighting method, which is calculated by query vector and key-value pair [29].

The context vector $d_j$ can be computed from $h_{jm}$ and $\alpha_j$, as shown in the following equation:

$$d_j = \alpha_j h_{jm} \qquad (7)$$

where at the time $j$ ( $j=1,2,\ldots,n$ , and $n$ is the length of the input time sequence), $h_{jm}$ is the hidden output of the encoder, $\alpha_j$ is the key vector corresponding to the input. $\alpha_j$ can be calculated by the following equation:

$$\alpha_j = \frac{\exp(e_{jn})}{\sum_{j=1}^{n} \exp(e_{jn})} \qquad (8)$$

wherein $e_{jn}$ can be computed from the corresponding equation:

$$Q = \tanh(h_n W_q) \qquad (9)$$

$$K_j = \tanh(h_j W_k) \qquad (10)$$

$$e_{jn} = \frac{K_j Q^T}{\sqrt{m}} \qquad (11)$$

where $K_j$ is the attention score, $Q$ is the query vector, $e_{jn}$ is the similarity between the $j$th key vector and query vector, $m$ is the hidden size of the encoder, $h_j$ is the hidden state of the encoder at time $j$, $W_k$ and $W_q$ are the attention weight matrices randomly generated with a normalized Gauss distribution.

## 2.3 AttLSTM neural network model for satellite clock bias prediction

Figure 3 shows the architecture of the attention mechanism-based LSTM (AttLSTM) neural network model proposed in this paper:
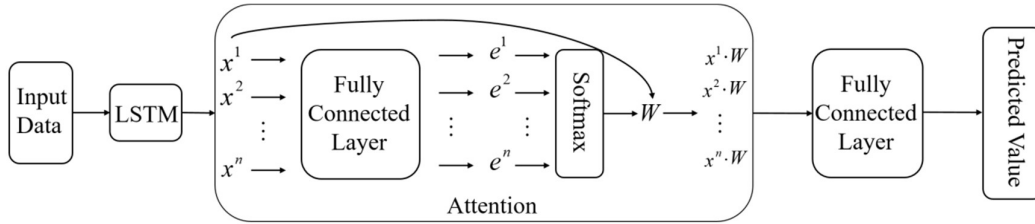


**Fig. 3 the architecture of AttLSTM model**

The architecture of AttLSTM model mainly includes the preprocessing of input data, the LSTM neural network layer, the attention mechanism layer, the fully connected layer and the prediction value output. AttLSTM performs attention mechanism on the output data of the LSTM layer considering the influence of the adjacent epoch on the satellite clock bias at the current time. A fully connected layer is constructed by a linear transformation function and predicted.

Time series prediction includes one-step prediction and multi-step prediction. One-step prediction refers to predicting only one value in each prediction, while multi-step prediction refers to predicting multiple values in each prediction, and the prediction error of multi-step prediction accumulates as the number of steps increases. Therefore, there is a serious error accumulation problem in multi-step prediction, and the data needs to be processed to make it a one-step prediction problem. Hence, data preprocessing is required

*Relu()* activation function, and the weight matrix $W$ is obtained by using the *Softmax()* function. The initial sample of the input and the weight vector are multiplied to obtain the new sample, and finally the output of the attention mechanism layer is obtained. After that, a fully connected layer is constructed to convert the output of the attention mechanism layer into the target value to be

before training with the AttLSTM model. The specific process is as follows: 1) Data single difference processing: It means taking difference of the data between epochs, that is, subtracting the previous data from the current data. It can eliminate possible systematic errors in the original clock bias sequence to a certain extent, which is conducive to the fitting and prediction of clock bias data. 2) Construct satellite clock bias time series input data: The clock bias data $\{y_1, y_2, \cdots y_n\}$ after single difference is constructed as $m$ time series with vector dimension $l$, where the length of the time

series $n$ is $n = m + l - 1$. 3) Data scaling and constructing supervised learning data: The constructed input $m$ time series are normalized and mapped to the target range [-1,1], which can improve the accuracy and convergence speed of the model. In each constructed time series of length $l$, the last data is used as the label for training, making it a one-step prediction problem. Finally, the sequence of the predicted clock bias is obtained by inverse transformation of the obtained output values.

Considering the efficiency and accuracy of the model, the input vector dimension parameter $l$ is set to 20 in the experiment. In the training process, the model weight is initialized by random initialization method, the learn rate is 0.01, the epoch is 1000, and the batch size is 64. Adam optimizer is used in the model because it can replace the traditional stochastic gradient descent algorithm. It has the advantages of computational efficiency and can realize the adaptive adjustment of learning rate. The evaluation function uses the root mean square error.

## 3. Prediction precision analysis

In order to study the satellite clock bias prediction accuracy of AttLSTM model, the MGEX precision clock products provided by German Research Centre for Geoscience (GFZ) are used to conduct the BDS-3 satellite clock bias prediction experiment. The time span of the data is from November 16, 2022 to November 19, 2022 with 30 s sampling interval. In the experiment, the one-day BDS-3 satellite clock bias is used as the training data, and the next day's 12 hours (12h) and 24 hours (24h) satellite clock bias are predicted. AttLSTM model is compared with LSTM model and QP model. The MGEX precision clock bias is used as the reference value, and the root mean square (RMS) error is used as the statistics of the prediction accuracy. The calculation formula for the RMS can be expressed as:

$$RMS = \sqrt{\frac{\sum_{i=1}^{n}(C_i - \hat{C}_i)(C_i - \hat{C}_i)}{n}} \qquad (12)$$

where $C_i$ is the predicted value of SCB at the moment $i$, and $\hat{C}_i$ is the reference value of SCB at the moment $i$.

Figures 4 and 5 show the comparison of the prediction accuracy of different models for each BDS-3 satellite under 12h and 24h prediction time, respectively.
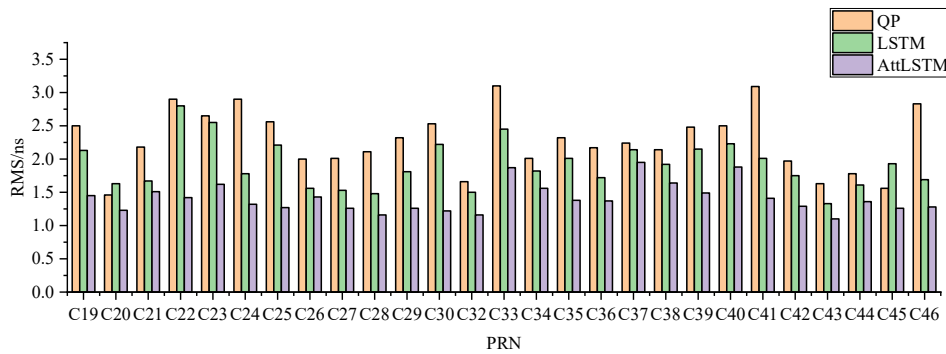


**Fig. 4 The mean prediction accuracy of the BDS-3 satellite clock bias of 12h**
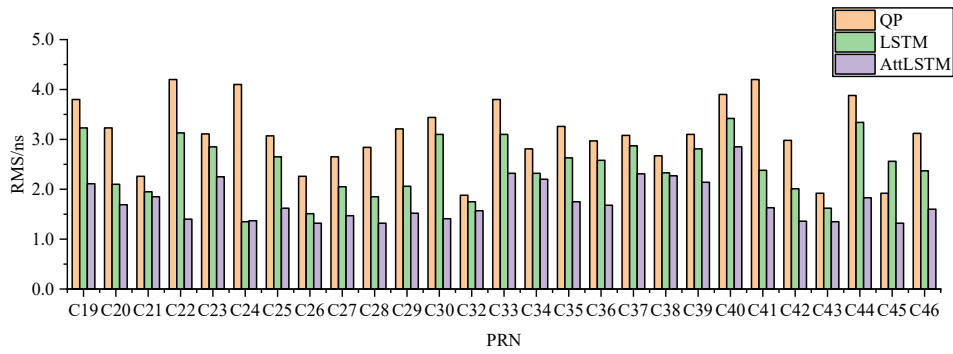
**Fig. 5 The mean prediction accuracy of the BDS-3 satellite clock bias of 24h**

According to the prediction accuracy of different models in Figures 4 and 5, AttLSTM model has the best prediction accuracy for each satellite, and in most cases significantly better than LSTM model and QP model. In addition, the change of RMS predicted by AttLSTM model for each satellite is more stable, while the change of RMS predicted by LSTM model and QP model for different satellites is larger. At the same time, with the increase of prediction time, AttLSTM model can still maintain

high prediction accuracy, which is better than LSTM and QP models, and has high stability.

The prediction residual values reflect the prediction accuracy, and the greater deviation from 0 indicates the worse prediction result. In this paper, the prediction residual values of four satellites C22 (rubidium clock), C39 (hydrogen clock), C41 (hydrogen clock) and C45 (rubidium clock) are selected for analysis, and they are shown in Figure 6.
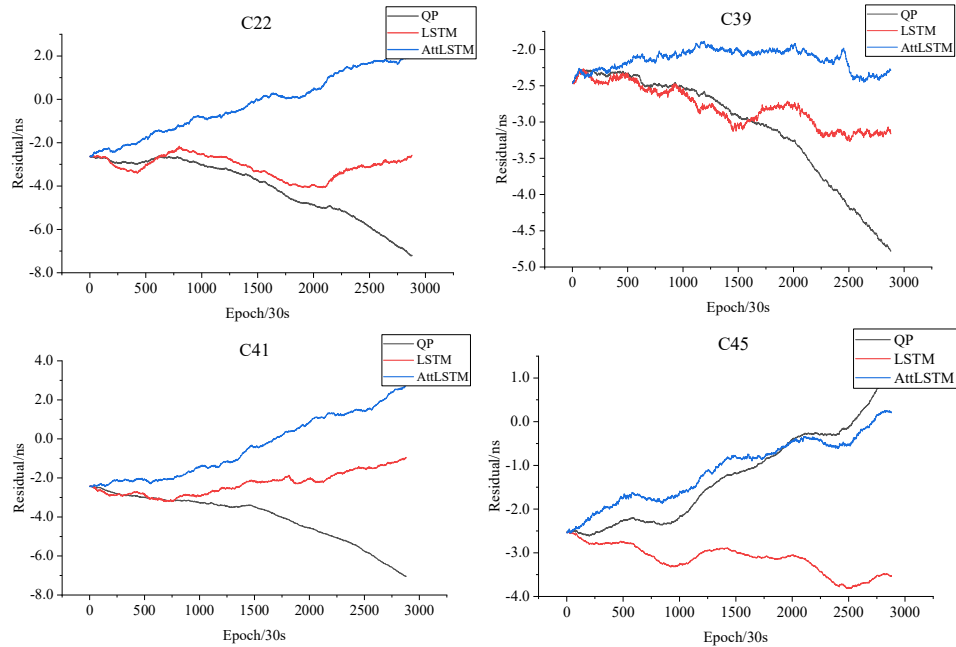


**Fig. 6 Residual diagram of 4 satellites predict of 24h**

Figure 6 shows that the residuals predicted by AttLSTM, LSTM and QP models for the four satellites clock bias have different changes. The residuals predicted by AttLSTM model of the four satellites clock bias are closer to 0, which is closer

to the reference value of the clock bias. However, LSTM and QP models deviate more from the reference value than AttLSTM model, and the deviation degree of LSTM and QP models is different due to the influence of different satellites.

To analyze the prediction accuracy of the models, the mean prediction accuracy of BDS-3 satellite equipped with the passive hydrogen maser (PHM) and rubidium atomic frequency (RAF) is calculated in this paper, as shown in Table 1:

**Table 1 Statistics of the prediction accuracy /ns**

| Types of atomic | 12h | | | 24h | | |
|---|---|---|---|---|---|---|
| | QP | LSTM | AttLSTM | QP | LSTM | AttLSTM |
| RAF | 2.37 | 2.0 | 1.45 | 3.12 | 2.57 | 1.80 |
| PHM | 2.23 | 1.84 | 1.38 | 3.05 | 2.40 | 1.73 |
| Mean | 2.29 | 1.91 | 1.41 | 3.08 | 2.47 | 1.75 |

Analysis of the statistical results in Table 1 shows that:

1) In the 12h and 24h prediction experiments, the proposed AttLSTM model has higher prediction accuracy than LSTM and QP models, while LSTM model has higher prediction accuracy than QP model. With the increase of prediction time, the error will gradually accumulate and the prediction accuracy will decrease with the increase of time.

2) The prediction accuracy of SCB is related to the different types of satellite atomic clocks as well. In the 24h prediction experiment, the average prediction accuracy of the hydrogen clock under the QP model, LSTM model and AttLSTM model reaches 3.05ns, 2.40ns and 1.73ns, while the rubidium clock reaches 3.12ns, 2.57ns and 1.80ns respectively. It can be seen that the prediction accuracy of the satellite equipped with hydrogen clock is slightly better than that of the rubidium clock.

3) In the prediction experiment of 12h, the averaged prediction accuracy of AttLSTM model is 1.41ns, which is 26.1% and 38.4% higher than LSTM and QP models, respectively. Besides, in the prediction experiment of 24h, the averaged prediction accuracy of AttLSTM model is 1.71ns, which is 29.1% and 43.1% higher than LSTM and QP models, respectively. It shows that the AttLSTM model proposed in this paper can greatly improve the prediction accuracy of SCB. Moreover, with the increase of prediction time, the prediction accuracy of AttLSTM model is better than that of the LSTM and QP models.

## 4. Positioning results and analysis

In order to verify the availability and accuracy of AttLSTM, LSTM and QP models in PPP, these three models are applied to 24h BDS-3 satellite clock bias prediction, and 15 MGEX stations are selected for static PPP experiments on November 17, 2022. The distribution of these stations is shown in Figure 7. The MGEX precise orbit products are used and the clock bias predicted by these models are chosen separately in PPP for all selected MGEX stations. The detailed PPP processing model is summarized in Table 2.
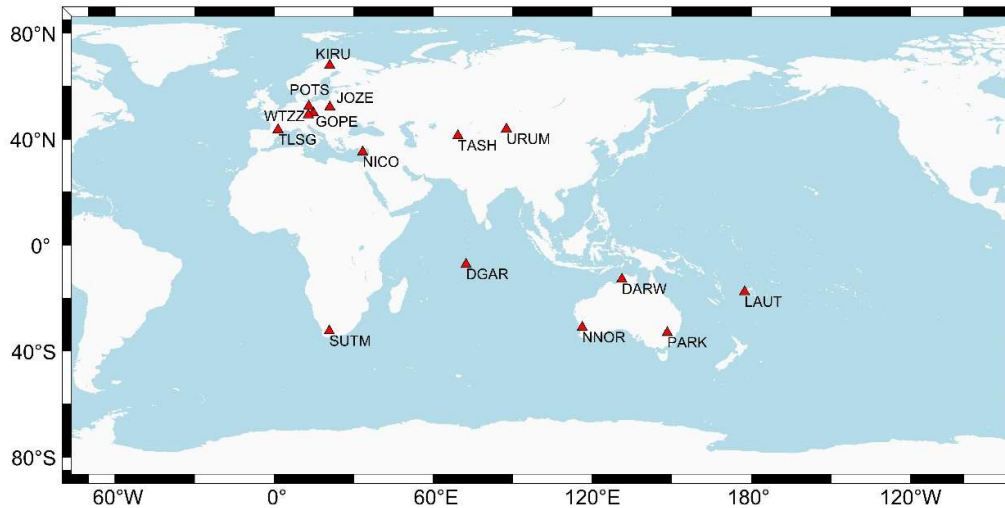
**Fig. 7 Distribution of selected 15 stations**

The precise coordinates from the SINEX solutions are used as references for PPP performance analysis to obtain the positioning errors of each station in the East, North, and Up directions. In order to intuitively analyze the influence of prediction clock bias on positioning, the static PPP positioning errors of NNOR and PARK stations are selected for analysis on November 17, 2022 (Figures 8 and 9).

Figures 8 and 9 show the static PPP positioning results of NNOR and PARK stations, and indicate the convergence time of the three prediction models in East, North, and Up directions can basically be between 1.5h and 4h. In terms of positioning accuracy, the RMS values of positioning errors in East, North, and Up directions of the AttLSTM model based on NNOR and PARK stations are better than those of the LSTM and QP models, and the deviation degree of the error curve from 0 value after convergence is smaller.

The positioning errors after the convergence of the static PPP of the selected 15 MGEX stations are counted, and the statistical results of the positioning accuracy of each station based on different clock bias prediction models in the East, North, and Up directions are shown in Figure 10. According to the comparison of three models in Figure 10, it can be said that AttLSTM model performs better than LSTM model and QP model in positioning in the East, North and Up directions among the 15 selected stations. Additionally, due to the positioning results of different stations, the positioning errors of different stations in the Up direction fluctuate greatly, and the error is larger than that in the East and North directions. For further analysis of the positioning results, the errors of all stations in the East, North, and Up directions after convergence, as well as the averaged 2D RMS and 3D RMS values, are counted and the results are shown in Table 3.

**Table 2 Strategies for BDS-3 satellites PPP**

| Items | Correction model or estimation |
|---|---|
| Satellites | BDS-3 satellites |
| Observations | Ionosphere-free code and |
| Cutoff elevation | 10° |
| Satellite orbit and | Fixed |
| PCO/PCV | Corrected with igs14.atx |
| Relativistic effects | Corrected |
| Solid tide | IERS 2010 |
| Ocean loading | IERS 2010 |
| Pole tide | IERS 2010 |
| Ionospheric delay | Ionosphere-free |
| | Saastamoinen model for dry |
| Tropospheric delay | delay and estimation for wet |
| | component |
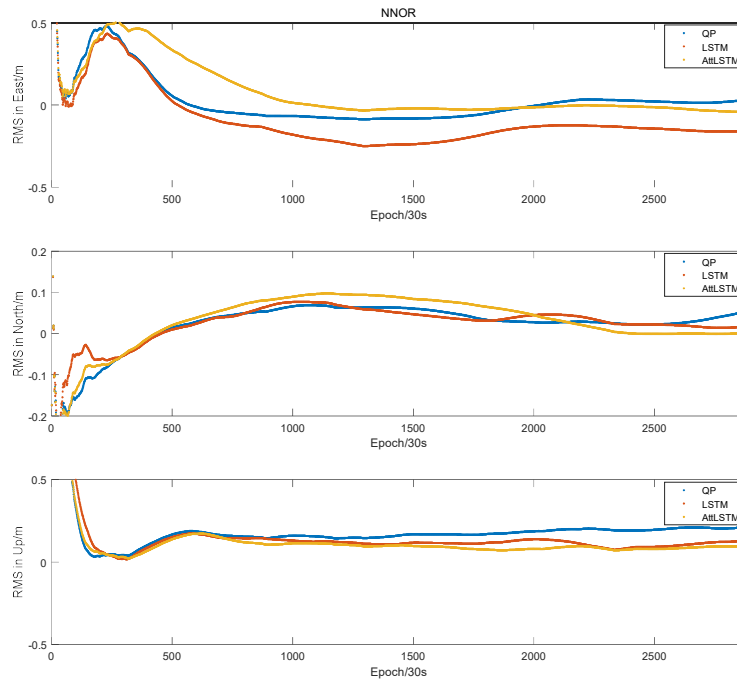
**Fig. 8 Static PPP positioning results of clock bias predicted by three models of NNOR station**
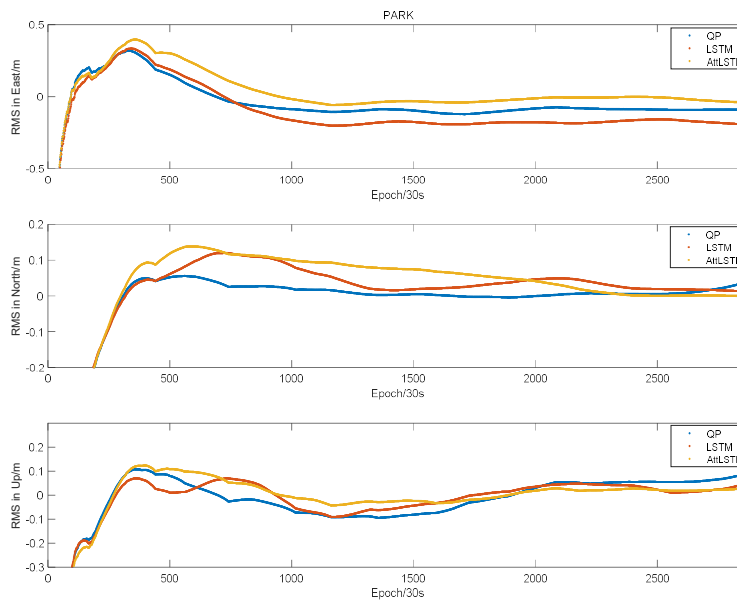


**Fig. 9 Static PPP positioning results of clock bias predicted by three models of PARK station**
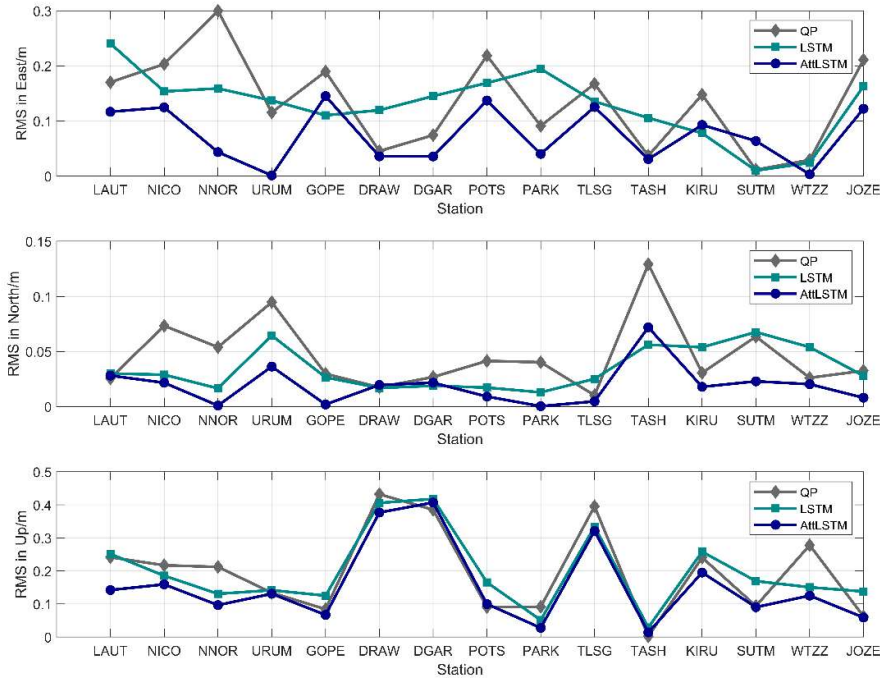
**Fig. 10 The RMS results of static PPP positioning errors based on three models in East, North and Up directions (top to bottom)**

Table 3 shows the averaged RMS values of the 15 MGEX stations under AttLSTM, LSTM, and QP models. The averaged RMSs of AttLSTM model in the East, North and Up directions can reach 0.074m, 0.019m and 0.154m, respectively, while the averaged 2D RMS reaches 0.077m, and the averaged 3D RMS reaches 0.172m. These results indicate that the averaged positioning accuracy under the AttLSTM model is higher than that of LSTM and QP models. Additionally, compared with LSTM and QP models; the averaged RMS in the East direction is improved by about 42.5% and 44.4%, the averaged RMS in the North direction is improved by about 44.7% and 58.9%, and the averaged RMS in the Up direction is improved by about 21.7% and 21.8%, while the 2D RMS is improved by about 41.3% and 45.8%, and the 3D RMS is improved by about 27.4% and 29.1%. In general, the accuracy improvement of AttLSTM model in East and North directions is significantly better than that in Up direction. Between the LSTM and QP models, the positioning accuracy of LSTM model is better than that of QP model in the East and North directions, while both have comparable positioning accuracy in the Up direction.

Considering both 2D and 3D RMSs, the positioning accuracy of LSTM model is better than QP model.

**Table 3 The averaged RMSs of positioning errors of fifteen stations for three prediction models**

| prediction models | RMS/m | | | | |
|---|---|---|---|---|---|
| | East | North | Up | 2D | 3D |
| QP | 0.134 | 0.046 | 0.197 | 0.142 | 0.243 |
| LSTM | 0.129 | 0.034 | 0.196 | 0.132 | 0.237 |
| AttLSTM | 0.074 | 0.019 | 0.154 | 0.077 | 0.172 |

## 5. Conclusions

In order to improve the prediction accuracy of satellite clock bias, an attention mechanism-based long short-term memory neural network (AttLSTM) model is applied to SCB prediction in this paper. Because adding an attention layer to the model, can make the model pay attention to the relative importance of each feature in the input data, and adaptively extract the influence weight of the historical clock bias data on the current time clock bias data to improve the prediction accuracy of the

model. Therefore, the clock bias prediction accuracy of AttLSTM, LSTM and QP models are compared and analyzed by using MGEX BDS-3 satellite precision clock product. Moreover, the predicted clock bias using the three models is applied to static PPP positioning respectively.

The experiment results show that the averaged prediction accuracy of the AttLSTM model for 12h and 24h can reach 1.41ns and 1.75ns, which are better than the LSTM and QP models. With the increase of the prediction time, the advantage of the AttLSTM model is more obvious. The prediction accuracy of the clock bias model is affected by the type of onboard atomic clock, too. Under the three models, the clock bias prediction accuracy of the BDS-3 satellite equipped with the hydrogen clock is slightly better than the rubidium clock. In the static PPP experiment of 15 MGEX stations, the averaged positioning accuracy of the AttLSTM model in East, North and Up directions can reach 0.074m, 0.019m and 0.154m respectively, which shows that the AttLSTM model also performs better than LSTM and QP models in static PPP. Compared with the LSTM model and QP model, it has a great improvement.

AttLSTM is a neural network model based on deep learning framework, which is suitable for time series prediction. In BDS-3 satellite clock bias prediction, AttLSTM model shows its advantages, and has a positive impact on reducing positioning error, which provides a new possibility/opportunity for improving the navigation satellite clock bias prediction accuracy. It is also expected to be used in precise orbit determination or other GNSS prediction problems. Due to the characteristics of the neural network model, different network structures, sample dimensions and different hyper-parameters will have a certain impact on the prediction results. Therefore, in practical applications, the model should be adjusted and verified in combination with different scenarios.

## References

[1] Ge H, Li B, Wu T, et al. (2021) Prediction models of GNSS satellite clock errors: Evaluation and application in PPP. Advances in Space Research, 68(6): 2470-2487.

[2] Li X, Ge M, Douša J, et al. (2014) Real-time precise point positioning regional augmentation for large GPS reference networks. GPS Solutions, 18(1): 61-71.

[3] Elsobeiey M, Al-Harbi S. (2016) Performance of real-time precise point positioning using IGS real-time service. GPS Solutions, 20(3): 565-571.

[4] El-Mowafy A, Deo M, Kubo N. (2017) Maintaining real-time precise point positioning during outages of orbit and clock corrections. GPS Solutions, 21(3): 937-947.

[5] Wang Y, Lu Z, Qu Y, et al. (2017) Improving prediction performance of GPS satellite clock bias based on wavelet neural network. GPS Solutions, 21(2): 523-534.

[6] Nie Z, Gao Y, Wang Z, et al. (2017) An approach to GPS clock prediction for real-time PPP during outages of RTS stream. GPS Solutions, 22(1): 14.

[7] Hadas T, Bosy J. (2015) IGS RTS precise orbits and clocks verification and quality degradation over time. GPS Solutions, 19(1): 93-105.

[8] Zhang L, Yang H, Yao Y, et al. (2019) A new datum jump detection and mitigation method of real-time service (RTS) clock products. GPS Solutions, 23(3): 67.

[9] He K, Weng D, Ji S, et al. (2020) Ocean real-time precise point positioning with the BeiDou short-message service. Remote Sensing, 12(24): 4167.

[10] LI H, LI X, GONG X. (2022) Improved method for the GPS high‑precision real‑time satellite clock error service. GPS Solutions, 26(4): 136.

[11] Huang G, Cui B, Zhang Q, et al. (2018) An improved predicted model for BDS ultra-rapid

satellite clock offsets. Remote Sensing, 10(1): 60.

[12] Liang Y, Ren C, Yang X, et al. (2015) Grey model based on first difference in the application of the satellite clock bias prediction. Acta astronomica sinica, 56(3): 264-277.

[13] Huang G, Zhang Q. (2012) Real-time estimation of satellite clock offset using adaptively robust Kalman filter with classified adaptive factors. GPS solutions, 16: 531-539.

[14] Lv D, Liu G, Qu J, et al. (2022) Prediction of GPS satellite clock offset based on an improved particle swarm algorithm optimized BP neural network. Remote Sensing, 14(10):2407.

[15] Gao Y, Chen G, Fu W, et al. (2023) A real-time linear prediction algorithm for detecting abnormal BDS-2/BDS-3 satellite clock offsets. Remote Sensing,15(7):1831.

[16] Huang G, Zhang Q, Xu G. (2014) Real-time clock offset prediction with an improved model. GPS solutions, 18(1): 95-104.

[17] Xu B, Wang Y, Yang X. (2013) Navigation satellite clock error prediction based on functional network. Neural processing letters, 38(2): 305-320.

[18] Ding Z, He K, Li M, et al. Comparative analysis of data quality and performance index forBDS-3 constellation. Journal of Global Positioning Systems, 2022, 18(01): 41-55.

[19] Wang Y, Lu Z, Qu Y, et al. (2017) Improving prediction performance of GPS satellite clock bias based on wavelet neural network. GPS solutions, 21(2): 523-534.

[20] He S, Liu J, Zhu X, et al. (2023) Research on modeling and predicting of BDS-3 satellite clock bias using the LSTM neural network model. GPS Solutions, 27(3): 108.

[21] Zhang S, Chen Y, Xiao J, et al. (2021) Hybrid wind speed forecasting model based on multivariate data secondary decomposition approach and deep learning algorithm with attention mechanism. Renewable Energy, 174: 688-704.

[22] Li Y, Zeng J, Shan S, et al. (2018) Occlusion aware facial expression recognition using CNN with attention mechanism. IEEE Transactions on Image Processing, 28(5): 2439-2450.

[23] Li T, Pan Y, Tong K, et al. (2021) A multi-scale attention neural network for sensor location selection and nonlinear structural seismic response prediction. Computers & Structures, 248: 106507.

[24] Cui M, Wu G, Chen Z, et al. (2021) Geometric attention regularization enhancing convolutional neural networks for bridge rubber bearing damage assessment. Journal of Performance of Constructed Facilities, 35(5): 04021061.

[25] Liu Y, Liu P, Wang X, et al. (2021) A study on water quality prediction by a hybrid dual channel CNN-LSTM model with attention mechanism. In International Conference on Smart Transportation and City Engineering, 12050: 797-804

[26] Yu Y, Si X, Hu C, et al. (2019) A review of recurrent neural networks: LSTM cells and network architectures. Neural computation, 31(7): 1235-1270.

[27] Cai K, Shen Z, Luo X, et al. (2023) Temporal attention aware dual-graph convolution network for air traffic flow prediction[J]. Journal of Air Transport Management, 106: 102301.

[28] Chen M, Zang S, Ai Z, et al. (2023) RFA-Net: Residual feature attention network for fine-grained image inpainting. Engineering Applications of Artificial Intelligence, 119: 105814.

[29] Liao Y, Lin R, Zhang R, et al. (2023) Attention-based LSTM (AttLSTM) neural network for seismic response modeling of bridges. Computers & Structures, 275: 106915.

## Authors

**Jiaxing Li** is a graduate student of

China University of petroleum (East China). His research focused on BDS-3 high-precision real-time positioning.

**Kaifei He** is a professor at the China University of Petroleum (East China). He received his Ph.D. degree in Geodesy from the Technical University of Berlin (TU Berlin) in 2015 and studied in GFZ as a Ph.D student from 2010 to 2014. Currently, his research focuses on GNSS navigation and positioning algorithms, underwater positioning, geodesy data processing, and software development.

**Tulay Kaya Eken** is an assistant professor at Bogazici University. She received her Ph.D. degree from Department of Earth and Planetary Science, Tokyo Institute of Technology in 2012. Currently her research focuses on analysis of geodetic and geophysical data for understanding of crustal deformation and geodynamic processes, and 2D and 3D inverse modeling.

**Haluk Özener** is a professor at Bogazici University. He received his Ph.D. degree from Bogazici University in 2000. Currently some of his research interests are analysis of geodetic data, crustal deformation monitoring, slip modeling, stochastic modelling, Geoinformation Systems/GIS applications, space geodesy.

**Xiang Xu** is a graduate student of China University of petroleum (East China). His research focused on GNSS/INS integrated navigation filtering algorithm.

**Xiaopeng Lu** received his Master degree in Geodesy and Survey Engineering from Chang'an

University in 2010. He is a nationally registered surveyor and senior engineer, mainly engaged in the construction of digital urban geographic spatial frameworks and GNSS data processing.

**Kai Ding** is a lecturer at Shandong Vocational College of Information Technology. He received his Master degree in Geodesy and Survey Engineering from Shandong University of Science and Technology in 2010. Currently, his research focuses on GNSS data processing and UAV mapping.

**XuChen Ma** is a graduate student of China University of petroleum (East China). His research focused on Multi-system high-precision dynamic real-time positioning.